Published in final edited form as:
Biomaterials. 2014 January ; 35(1): 14–24. doi:10.1016/j.biomaterials.2013.09.059.

PHACOS, a functionalized bacterial polyester with bactericidal activity against methicillin-resistant *Staphylococcus aureus*

Nina Dinjaski[a], **Mar Fernández-Gutiérrez**[b,f], **Shivaram Selvam**[c,d], **Francisco J. Parra-Ruiz**[b,f], **Susan M. Lehman**[c,d], **Julio San Román**[b,f], **Ernesto García**[a,e], **José L. García**[a], **Andrés J. García**[c,d], and **María Auxiliadora Prieto**[a,*]

[a]Centro de Investigaciones Biológicas, CSIC, Madrid 28040, Spain

[b]Instituto de Ciencia y Tecnología de Polímeros, CSIC, Madrid 28006, Spain

[c]Woodruff School of Mechanical Engineering, Georgia Institute of Technology, Atlanta 30332-0363, USA

[d]Petit Institute for Bioengineering and Bioscience, Georgia Institute of Technology, Atlanta 30332-0363, USA

[e]CIBER de Enfermedades Respiratorias (CIBERES), Spain[1]

[f]CIBER-BBN, Centro de Investigación Biomédica en Red Bioingeniería, Biomateriales y Nanomedicina, Spain

Abstract

Biomaterial-associated infections represent a significant clinical problem, and treatment of these microbial infections is becoming troublesome due to the increasing number of antibiotic-resistant strains. Here, we report a naturally functionalized bacterial polyhydroxyalkanoate (PHACOS) with antibacterial properties. We demonstrate that PHACOS selectively and efficiently inhibits the growth of methicillin-resistant *Staphylococcus aureus* (MRSA) both *in vitro* and *in vivo*. This ability has been ascribed to the functionalized side chains containing thioester groups. Significantly less (3.2-fold) biofilm formation of *S. aureus* was detected on PHACOS compared to biofilms formed on control poly(3-hydroxyoctanoate-*co*-hydroxyhexanoate) and poly(ethylene terephthalate), but no differences were observed in bacterial adhesion among these polymers. PHACOS elicited minimal cytotoxic and inflammatory effects on murine macrophages and supported normal fibroblast adhesion. *In vivo* fluorescence imaging demonstrated minimal inflammation and excellent antibacterial activity for PHACOS compared to controls in an *in vivo* model of implant-associated infection. Additionally, reductions in neutrophils and macrophages in the vicinity of sterile PHACOS compared to sterile PHO implant were observed by immunohistochemistry. Moreover, a similar percentage of inflammatory cells was found in the tissue surrounding sterile PHACOS and *S. aureus* pre-colonized PHACOS implants, and these levels were significantly lower than *S. aureus* pre-colonized control polymers. These findings support a contact active surface mode of antibacterial action for PHACOS and establish this functionalized polyhydroxyalkanoate as an infection-resistant biomaterial.

*Corresponding author. Centro de Investigaciones Biológicas, CSIC, Ramiro de Maeztu, 9, 28040 Madrid, Spain. Fax: +34 91 536 0432. auxi@cib.csic.es (M.A. Prieto).

[1]http://www.ciberes.org.

Keywords

Functionalized polyhydroxyalkanoate; Antimicrobial polymers; Methicillin-resistant *Staphylococcus aureus*; Biofilm; Biomaterial infection

1. Introduction

Bacterial infections are a major cause of morbidity and mortality worldwide and many infections can be attributed to *Staphylococcus* species [1]. The acute pathogenic properties of *Staphylococcus aureus* [2] as well as its ability to cause chronic infections and persist on medical implants or host tissues is recognized as a significant healthcare threat [3]. In fact, the ability of *S. aureus* to form biofilms has been linked to the persistence of chronic infections [1]. Methicillin-resistant *S. aureus* (MRSA), which have developed resistance to virtually all β-lactam antibiotics [4], are a major concern. MRSA are especially troublesome in hospitals, prisons, schools, and nursing homes where patients with open wounds, invasive devices, and/or weakened immune systems are at high risk of infection [5].

Although the bactericidal properties of some polymers were reported as early as in 1965 [6], antimicrobial polymers represent a class of increasingly important materials that may represent an alternative to current biocides and, in some cases, even to antibiotics. In the past decade, the number of Food and Drug Administration (FDA)-approved disinfecting polymers has significantly increased, supporting the compelling need for alternatives to antibiotics and environmentally critical disinfectants [7]. Antimicrobial surfaces that prevent growth of biofilms are considered an effective strategy to inhibit the establishment and spread of microbial infections. Such surfaces either repel microbes – so they cannot attach to it – or kill them in their vicinity [7].

Most polymeric and biodegradable systems currently used in medicine are based on poly(lactic acid), poly(glycolic acid) and on their copolymers [8]. One of the leading candidates with potential applications in the medical field is the group of naturally produced bacterial polyesters or poly([*R*]-3-hydroxyalkanoates) (PHAs) that constitute a large class of biodegradable biopolymers that show minimal tissue toxicity [9]. The physical and mechanical properties of PHAs are significantly influenced by their monomer composition and chemical structure [10]. Some short-chain-length PHAs may be too rigid and brittle and lack the superior mechanical properties required for biomedical and packaging film applications. In contrast, medium-chain-length PHAs (mcl-PHAs) may be elastomeric but have very low mechanical strength. Therefore, the physical and mechanical characteristics of microbial polyesters need to be diversified and improved for packaging materials, tissue engineering, and other specific applications [11,12].

Recently, we produced poly-3-hydroxy-acetyllthioalkanoate-*co*-3-hydroxyalkanoate (PHACOS), a new second generation polymer containing thioester groups in the side chain (Fig. 1a) [13]. In this work, we analyzed the antimicrobial properties of PHACOS compared to the non-reactive poly(3-hydroxyoctanoate-*co*-hydroxyhexanoate) (PHO) and poly(ethylene terephthalate) (PET) in *in vitro* and *in vivo* models.

2. Materials and methods

2.1. Polymer preparation, disk fabrication, and endotoxin analysis

PHACOS and PHO polymers (Fig. 1) were prepared as previously reported [13] and kindly provided by Biópolis, S.L. To determine the monomer composition of PHA, gas chromatography-mass spectrometry and nuclear magnetic resonance analyses were carried

out [13]. The monomer content of PHACOS was 29.7% of non-functionalized monomers [17.5% of 3-hydroxyoctanoate (OH-C8), 10.3% of 3-hydroxydecanoate, and 1.9% of 3-hydroxyhexanoate (OH-C6) monomers] and 70.3% of functionalized monomers (46.4% of 3-hydroxy-6-acetylthiohexanoate and 23.9% of 3-hydroxy-4-acetylthiobutanoate monomers). PHO consisted of 8.5% OH-C6 and 91.5% OH-C8. An optimized downstream processing was applied to eliminate endotoxins [14]. Briefly, 1 g of PHA was dissolved in 100 mL of chloroform at 40°C under vigorous stirring, the suspension was pressure filtered and the polymer was precipitated by addition of non-solvent methanol. Finally, the polymer was dried under vacuum at 40 °C for 48 h. This procedure was repeated two times to obtain mcl-PHA with endotoxin units (EU) ≤20 EU g^{-1}, in compliance with the endotoxin requirements for biomedical applications [15]. The endotoxin content was measured using a *Limulus* amebocyte lysate (LAL)-test (Pyrogent Plus Single Test Kit, Lonza). The values of PHACOS and PHO endotoxicity were <12 EU g^{-1} and <15 EU g^{31}, respectively.

Poly(ethylene terephthalate) (PET) disks were coated with PHACOS or PHO by solvent-casting. Polymeric materials dissolved in chloroform (2% w/v) were applied over sterile, endotoxin-free PET disks (6 mm diameter; kindly supplied by ACCIONA, Barcelona, Spain), in a dust-free atmosphere. The coatings were allowed to dry for 72 h at room temperature and the resulting PHACOS-coated disks (PHACOS disks), PHO-coated disks (PHO disks) and control PET disks were sterilized with ethylene oxide at 40 °C.

2.2. Bacterial strains, media and pre-culture suspensions

The bacterial strains used in this study are listed in Table 1. Bacteria were transferred from a frozen stock (−80 °C in 15% of glycerol) to screw-capped test tubes containing nutrient agar (Nutrient Broth Difco™, NB, supplemented with 1.5% agar) and incubated at 37 °C for 16–24 h. Afterwards, bacteria were transferred onto fresh slant culture medium and incubated at 37 °C for 16–20 h. These were designated hereafter as “pre-cultured bacteria”. The phenotypes including the MICs to resistance to common antibiotics of *S. aureus* (MRSA) are shown in Table S1.

2.3. Biofllm formation on mcl-PHAs

To determine the capacity of polymers to prevent bacterial biofilm formation, *S. aureus*^{T} and *Pseudomonas aeruginosa* CECT 4122 were used. Pre-cultured bacteria were incubated in trypticase soy broth (TSB) supplemented with 0.3% glucose and 0.4% yeast extract (enriched TSB or e-TSB) with shaking, at 37 °C for 20 h. Bacterial concentration was estimated spectrophotometrically at 600 nm. Biofilm formation was carried out (in triplicate) as follows: endotoxin-free, sterile PHO disks, PHACOS disks or control PET disks were placed in 24-flat bottom well plates (Falcon, Becton Dickinson) and each well was inoculated with 1 mL of a 1/100 dilution in TSB of a saturated culture previously grown in e-TSB. Plates were incubated under static conditions for 16 h at 37 °C and bacterial growth was determined by measuring the optical density at 595 nm (OD_{595}) using a plate reader (microplate absorbance reader 2020; Anthos Labtec Instruments GmbH). The ability of bacteria to form biofilms was analyzed by environmental scanning electron microscopy (ESEM), crystal violet staining [16], and colony-forming units (CFU) counting.

ESEM was employed to examine the formation of biofilm on PHACOS, PHO and PET control disks. Disks were washed three times with distilled sterile water and fixed with 2.5% glutaraldehyde for 2 h at room temperature. The dried samples were mounted on aluminum stumps and sputter-coated with chromium before examination under an ESEM apparatus (Philips XL 30) at an accelerating voltage of 15 kV.

For CFU counting, disks were washed with distilled water and the bacteria in the biofilms were mechanically removed from the disk using a disposable, sterile micropipette tip. CFU were determined by plating serial dilutions on Lysogeny Broth (LB) agar plates [17] and incubation at 37 °C for 24 h.

2.4. Bacterial adhesion to polymers

For adhesion experiments, inocula were prepared by suspending pre-cultured bacteria in 2 mL of 1/500 (v/v) diluted NB. Bacterial suspensions ($1–2 \times 10^8$ CFUs mL^{-1}) were placed on PHACOS, PHO and control PET disks and incubated at 37 °C for 24 h. After rinsing, adherent bacteria were stained with the LIVE/DEAD *Bac*Light bacterial viability kit L-13152 (Invitrogen-Molecular Probes) following the manufacturer's instructions. Samples were visualized with a Zeiss Axioplan Universal epifluorescence microscope operated for incident-light fluorescence and contrasting techniques of bright field and phase contrast. Micrographs were recorded with a digital camera Leica DFC350FX.

2.5. Measurement of the antimicrobial activity of PHACOS and PHO

Antibacterial activity was determined according to the ISO 22196:2011 protocol (http://www.iso.org/iso/catalogue_detail.htm?csnumber=54431), with minor modifications. Each disk was placed into a separate sterile Petri dish with the test surface facing up and wet filter paper beneath to maintain a relative humidity ≥90%. Test inoculums ($6.2–25.0 \times 10^3$ CFU cm^{-2}) prepared in 1/500 diluted NB were placed onto the polymers without cover film and incubated at 37 °C for 24 h. Each material was tested in triplicate. Non-coated PET disks were used as controls for determination of bacterial viability. Samples were analyzed at 0 h and 24 h. After incubation, disks were washed with 1 mL of phosphate-buffered saline, pH 7.2 (PBS). The number of colonies recovered from PET disks at 0 h was used to determine the recovery rate of the bacteria from the disks under investigation. Antibacterial activity was calculated as the R value. $R = 0.0$ means that the logarithm of number of viable cells in the sample disk after 24 h is identical to that of control disk at the same time point, whereas $R = 1.0$ means 10-fold less viable cells recovered from sample disk after 24 h compared with the control PET disk.

2.6. Determination of minimal inhibitory concentration (MIC)

The minimal inhibitory concentration (MIC) of polymer precursors 6-acetythiohexanoic acid (545554, Sigma–Aldrich), octanoic acid (C5038, Sigma– Aldrich) and hexanoic acid (P9767, Sigma–Aldrich) was determined by microdilution assays [18]. Stock solutions (60 mM) of each compound were prepared in PBS and serial dilutions were made in Muller-Hinton broth II (MHB II, Becton Dickinson).

2.7. In vitro cytocompatibility

2.7.1. Cell cultures—Cellular toxicity was evaluated using either murine RAW 264.7 macrophages (ECACC, Sigma P11) or BALB 3T3 fibroblasts (ATCC, CCL-163, P12), while inflammatory activity was monitored only on RAW 264.7 cells and effects on cell proliferation only on fibroblasts BALB 3T3. Cells were cultured in Dulbecco's modified Eagle's medium (DMEM) supplemented with HEPES (for BALB 3T3 cells) or sodium pyruvate (110 mg L^{-1}; for RAW 264.7 cells), and 10% fetal bovine serum (FBS), 100 units mL^{-1} penicillin, 100 μg mL^{-1} streptomycin and 200 mM L-glutamine (complete medium). A humidified atmosphere at 37 °C with 5% CO_2 and 95% of air was used for cell cultures growth.

2.7.2. MTT assay—The *in vitro* effects of products released from the polymers on cellular viability was assessed by the 3-(4,5-dimethylthiazol-2-yl)-2,5-diphenyltetrazolium bromide

(MTT) assay [19]. PHO, PHACOS or control PET disks were immersed in 5 mL of FBS-free DMEM and placed on a roller mixer at 37 °C. The medium was withdrawn at different time points and replaced with fresh medium. All these “extracts” were obtained under sterile conditions.

RAW 264.7 and BALB 3T3 cells were seeded at 2×10^5 cells mL^{-1} and 10^5 cells mL^{-1}, respectively, in a sterile 96-well culture plate and grown to confluence. The culture medium was replaced with the corresponding extract and incubated at 37 °C for 24 h in humidified air with 5% CO_2. Afterwards, cell viability was determined by adding MTT reagent (0.5 mg/mL in PBS) for 4 h at 37 °C. Excess medium and MTT reagent were withdrawn and dimethylsulfoxide was added to solubilize the formazan crystals formed in viable cells. The OD_{570} (test wavelength) and OD_{630} (reference wavelength) were determined using a microplate reader (Biotek SYNERGY-HT). Cell viability (CV) was calculated from equation: $CV\ (\%) = 100 \times (OD_S – OD_B)/OD_{C,}$ where OD_S, OD_B and OD_C are, respectively, the optical density of formazan production for the sample, blank (DMEM without cells), and control.

2.7.3. Griess assay—The inflammatory activity of polymers was investigated using a nitric oxide inhibitory assay [20]. Briefly, RAW 264.7 cells were seeded in 96-well plates at a density of 2×10^5 cells mL^{-1} and incubated at 37 °C for 24 h. After incubation, the corresponding extracts were added. Control wells received lipopolysaccharide (LPS) (1 mg mL^{-1}) and cells were incubated for 24 h. The nitrite concentration was determined by the Griess reaction [21]. Aliquots (100 μL) of the supernatant from RAW 264.7 cells were reacted with 100 μL of Griess reagent [1:1 mixture of 0.1% *N*-(1-naphthyl) ethylenediamine in water and 1% sulphanilamide in 5% phosphoric acid] in a 96-well plate and the OD_{548} was recorded. The nitrite concentration was calculated from a calibration curve previously obtained using known $NaNO_2$ concentrations. Data were expressed as the percentage of NO production.

2.7.4. Cell proliferation assay—The Alamar Blue (AB) assay was performed to monitor cell metabolic activity. BALB 3T3 cells were seeded at a density of 8×10^4 cells mL^{-1} over the disks placed in 24-well plates and grown for 24 h. To each specimen 1 mL of AB dye (10% AB solution in phenol red-free DMEM medium) was added and after 4 h of incubation 100 μL from each test sample was transferred to a 96-well plate to determine OD_{530} (excitation) and OD_{590} (emission). Then, to continue monitoring of cell growth disks were washed twice with PBS and 1 mL of culture medium was added. The assay was repeated at defined time points (1, 5 and 10 d).

2.7.5. Cell morphology—For determination of cell morphology, PHO, PHACOS and control PET disks were placed in a 24-well tissue-culture plate. BALB 3T3 cells (8×10^4 cells per well) were added and allowed to attach at 37 °C. Cell morphology was examined by ESEM (see above).

2.8. In vivo responses and anti-bacterial effects

2.8.1. Preparation of hydro-indocyanine green—Hydro-indocyanine green (H-ICG) was synthesized from ICG (Acros Organics) by reduction with sodium borohydride as described [22]. Briefly, 2 mg of dye was dissolved in 4 mL of methanol and reduced with 2–3 mg of sodium borohydride (Aldrich). The solvent was removed using a rotary evaporator (Rotavapor R-210, BUCHI Labortechnik AG, Switzerland). The dye was nitrogen capped and stored overnight at −20 °C. For bioimaging, the resulting solid was dissolved in sterile water to a final concentration of 1 mg mL^{-1} and filtered before use.

2.8.2. Sample preparation, implantation and bioimaging—Biomaterial disks were incubated for 30 min at 37 °C with the bacteria in 1/500 diluted NB (1×10^4 CFU cm^{-2}) under static conditions. After incubation, disks were placed in sterile containers.

National Institutes of Health (NIH) guidelines for the care and use of laboratory animals were followed [23]. All surgical procedures were approved by the Institutional Animal Care and Use Committee at the Georgia Institute of Technology. Sterile, endotoxin-free disks were implanted subcutaneously in the back of 6–8 weeks old male BALB/c mice (Jackson Laboratories) anesthetized by isofluorane. A single 1-cm incision was made on the dorsum proximal to the spine, and a subcutaneous pocket laterally spanning the dorsum was created. Sterile disks (two per mouse, one on either side of the spine) were implanted, and the incision was closed using sterile wound clips. Mice undergoing the same surgical procedure but receiving no biomaterial implants were used as sham controls to account for surgery-associated trauma/inflammation. The same procedure was followed for implants incubated with bacteria.

For bioimaging of reactive oxygen species associated with biomaterial-associated inflammation [24], 30 μL of H-ICG (1 mg mL^{-1} in sterile water) was injected near the vicinity of the implant at 1, 4 and 7 d post-surgery/implantation. Thirty minutes later, the whole body of the animal was scanned in an IVIS Lumina® bioimaging system (Xenogen). Biofluorescence was integrated using Living Image® software Version 3.1 (Xenogen).

2.8.3. Implant analysis—After euthanasia, disks were carefully explanted with the intact surrounding tissue to avoid disrupting the cell–material interface. For immunohistochemical staining, explants were embedded in optimal cutting temperature compound (Tissue-Tek) and cryosectioned at 10 μm. Fresh-frozen cryostat sections were incubated in 100 mM hydro-Cy5 (H-Cy5) for 45 min at 37 °C to stain for intra-cellular ROS. Afterwards, sections were fixed with 4% paraformaldehyde and stained with rat monoclonal antibodies (Abcam) against macrophage (CD68) or neutrophil (NIMP-R14) markers. Alexa Fluor 488-conjugated goat anti-mouse specific antibody (Invitrogen) was used as a secondary antibody. Sections were mounted with antifade mounting media containing 4′,6-diamidino-2-phenylindole (DAPI, Vector Labs) and imaged under a Nikon C1 imaging system. Five-six fields per sample were acquired and ImageJ software was used to count the fluorescent-labeled cells.

2.9. Statistical analysis

Statistical analysis was performed by two-way ANOVA using Tukey post-hoc test with $P \leq 0.05$ considered signisicant. For longitudinal ROS bioimaging studies, a two-way repeated measures ANOVA was used to account for the variance within subjects. Pair-wise comparisons were performed using Bonferroni post-hoc test with $P \leq 0.05$ considered significant.

3. Results

3.1. Biofilm formation by *S. aureus*^{T} on PHACOS

Previous studies had shown that the quality of bacterial biofilm on mcl-PHAs varies depending on both bacterial strain and purity of the material supporting biofilm formation [25]. Based on this observation, we focused on studying the ability of *S. aureus*^{T} and *P. aeruginosa* to form biofilms on PHACOS and PHO surfaces. ESEM showed less biofilm formed by *S. aureus*^{T} than *P. aeruginosa* on PHACOS at 16 h, while the biofilms formed by either strain on PHO were similar. However, adhered cells were always observed in both polymers (Fig. 2a). *S. aureus*^{T} formed 3-fold less biofilm than *P. aeruginosa* on PHACOS,

whereas the biofilm formed on PHO was similar for both strains, as shown by crystal violet staining (Fig. 2b). Moreover CFU counting confirmed these results, showing that the *S. aureus*^{T} biofilm on PHACOS contained 10% of the bacteria found in the *P. aeruginosa* biofilm (Fig. 2c). Additionally, PHACOS had significantly less *S. aureus*^{T} counts than PHO.

To determine whether the differences in biofilm formation on PHACOS resulted from differences in initial bacterial attachment, the number of adhered bacteria was analyzed by epifluorescence microscopy. In these experiments, bacteria were suspended in a 1/500 diluted NB medium and deposited on the PHACOS and PHO surfaces for 24 h. The lack of nutrients in the diluted suspension avoided biofilm formation but allowed testing the adhesion step of biofilm formation. There were no differences between the number of adherent *S. aureus*^{T} cells to PHO and PHACOS (Fig. 3a,b), but the number of *S. aureus*^{T} cells was lower than that of *P. aeruginosa* on both surfaces (PHO and PHACOS) (data not shown).

We next examined whether PHACOS was capable of bacterial killing using the LIVE/DEAD *Bac*Light™ kit (Fig. 3a,b). The percentage of viable *S. aureus*^{T} on PHACOS was much lower (20%) than those on PHO (83%), suggesting that PHACOS possesses anti-staphylococcal activity.

3.2. Antibacterial activity of PHACOS against MRSA

We further analyzed the antibacterial activity of PHACOS following ISO 22196:2011 standard protocol used to characterize the effectiveness of the antibacterial polymer. In these assays we compared the viability of nine Gram-positive and two Gram-negative bacteria (Table 1) after contacting the PHACOS surface. Susceptibility to PHACOS was evident only in some Gram-positive bacteria. Moreover, the antimicrobial activity of PHACOS was apparently restricted to *S. aureus* strains, including MRSA clinical isolates ($R \approx 1.03$) (Fig. 3c). However, when bacterial inocula exceeded 10^6 CFU cm^{-2}, no anti-staphylococcal activity could be detected (data not shown), which suggested that a direct contact between bacteria and the polymer is a prerequisite for PHACOS antimicrobial activity.

3.3. Antimicrobial activity dependence on thioester group

To examine whether the antimicrobial activity of PHACOS was due to the presence of thioester groups in the side chain of the polymer, the antimicrobial activity of fatty acids with structures similar to PHACOS monomers (octanoic, hexanoic and 6-acetylthiohexanoic acids) was studied using *S. aureus*^{T}. The MIC of 6-acetylthiohexanoic acid (40 μM) was 15-fold lower than that of hexanoic acid (0.7 mM). Moreover, octanoic acid was less harmful for staphylococci (MIC = 3 mM) than hexanoic acid (data not shown). These results suggested that thioester groups play a relevant role on the microbicidal activity of PHACOS.

3.4. In vitro mammalian cell adhesion properties and cytotoxicity of PHACOS

The viability and metabolic functions of mammalian cells in culture were measured using the MTT assay. This test is dependent on the intact activity of the mitochondrial succinate dehydrogenase that may be impaired after exposure of cells to toxic species. No detectable mitochondrial damage could be found for any of the tested surfaces as the viability of macrophages in presence of extracts prepared from the polymers was approximately 100% (Fig. 4a,b). Similarly, no changes in metabolic activity were detected among PET, PHO, and PHACOS for fibroblasts (Fig. 4c).

To measure the inflammatory activity of the polymers, a NO inhibitory assay was employed. NO is a mediator and regulator in many pathological reactions, especially in acute inflammatory responses [20]. Pro-inflammatory agents, such as LPS, increase NO

production in macrophages through activation of inducible NO synthase [26]. No differences in NO activity was measured for extracts from PHO and PHACOS compared to the PET control (Fig. 4d), even though the LPS positive control produced robust increases in NO activity. Finally, we examined whether PHACOS supports mammalian cell adhesion and proliferation using the Alamar Blue assay. PHACOS supported equivalent levels of cell activity as the PET control, whereas PHO supported reduced cell activity (Fig. 5). Moreover, the morphology and growth of fibroblasts was normal on all tested surfaces after 7 d (data not shown).

3.5. In vivo inflammatory responses and antibacterial activity

We have recently established the use of H-ICG to evaluate the production of ROS linked to implant-associated inflammation [24]. PET disks coated with either PHO or PHACOS were implanted subcutaneously in mice and we monitored ROS associated with inflammatory responses to implanted biomaterials via a single local injection of H-ICG dye at the vicinity of the surgical site. After 30 min animals were imaged via an IVIS fluorescence imaging system. Mice undergoing the same surgical procedure, but receiving no implants were used as sham controls to account for surgery-associated trauma/inflammation, whereas some mice received dye injection but no surgery (dye-only control). As expected, mice receiving biomaterial implants exhibited increases in fluorescence signal over time that were higher than the dye-only control (Fig. 6). Notably, no significant differences in fluorescence signals were observed among sterile PHACOS and PHO implants and the sham control. This result indicates minimal inflammation associated with these polymers.

We also examined whether PHACOS exhibits antimicrobial properties *in vivo*. After a short incubation with *S. aureus*^{T}, biomaterial disks were implanted subcutaneously as described above. Implant-associated inflammation was monitored using H-ICG and *in vivo* imaging. Significantly higher ROS signals were observed for PHO disks incubated with bacteria compared to sterile PHO disks (Fig. 6). These increased levels reflect the increased inflammatory response associated with the infected implant. Remarkably, PHA-COS disks incubated with bacteria exhibited significantly lower ROS signal compared to bacteria-incubated PHO disks, and the ROS levels for bacteria-incubated PHACOS disks were not different from the levels for sterile PHACOS implants. Taken together, these results demonstrate that PHACOS effectively controls biomaterial-associated infections by *S. aureus* in an *in vivo* model of device-related infection.

Following imaging, mice were sacrificed and the disks were retrieved along with implant-associated tissues. Using immunohistochemistry, we analyzed macrophage (CD68^{+}, green) and neutrophil (NIMP-R14^{+}, green) recruitment to the implant (Fig. 7a,c). Additionally, total cell number (DAPI stained, blue) was compared with the number of inflammatory cells (Fig. 7a,c,e). Higher recruitment of inflammatory cells was found to the vicinity of the sterile PHO implants (76% of total cell number) compared with sterile PHACOS implants (62% of total cell number) at 14 d post-implantation. Moreover, when the implants were pre-colonized with *S. aureus*^{T}, the influx of inflammatory cells was higher in the vicinity of the PHO implant (82% of total cell number) than around PHACOS implant (65% of total cell number). It is worth noting that there was a statistically significant difference ($P < 0.05$) between macrophage recruitment to *S. aureus*^{T} pre-colonized PHO (38% macrophages) and *S. aureus*^{T} pre-colonized PHACOS (31% macrophages) implant. Remarkably, there was no statistically significant difference ($P = 0.05$) in macrophage recruitment between *S. aureus*^{T} pre-colonized PHACOS (31% macrophages) and sterile PHACOS implants (29% macrophages). Moreover, significant differences ($P < 0.05$) in neutrophil recruitment to sterile PHO (43% neutrophils) and sterile PHACOS (33% neutrophils) implants, as well as between *S. aureus*^{T} pre-colonized PHO (44% neutrophils) and *S. aureus*^{T} pre-colonized

PHACOS implants (34% neutrophils) were observed. Taken together, obtained results indicate mild inflammatory response to sterile PHACOS implant and its antimicrobial effectiveness *in vivo*.

In addition, we co-stained for intracellular ROS activity using hydro-Cy5 (H-Cy5) as previously described [27]. Importantly, co-staining analysis for inflammatory cell markers and ROS activity demonstrated that neutrophils and macrophages are primarily responsible for the ROS activity associated with the implant (Fig. 7b,c). As expected, neutrophils are mainly responsible for ROS activity, when the implants are pre-colonized with *S. aureus*^{T} (Fig. 7f).

4. Discussion

Biomaterial-related infections represent a growing healthcare problem [28], as bacterial colonization and biofilm development can be prelude to both systemic infection and malfunction of implanted device. An additional confounding problem is an increasing incidence of multi-drug resistant bacteria (also known as “superbugs”). Decrease in the number of effective antibiotics, as well as the slower pace of development of new antibiotics to replace those that become ineffective is an emerging threat to public health [29]. In addition, current actions to prevent antimicrobial resistance are not sufficient. Tremendous efforts have focused on developing compounds that, not only show high efficacy, but also are less susceptible to resistance development in the bacteria. The high incidence and rapid emergence of resistance to antibiotics in various Gram-positive cocci makes Gram-positive pathogens a major health hazard. In addition, Klein et al. [5] reported that during 1999–2006 the percentage of MRSA increased >90%, or ≈ 10% a year, in outpatients admitted to US hospitals. The development of newer, stronger antibiotics which can overcome these acquired resistances is still a scientific challenge because new modes of antimicrobial action are required. Antimicrobial polymers have emerged as a promising candidate for further development as antimicrobial agents with decreased potential for resistance development [30].

We explored the possibilities of applications as biomedical devices made of the recently synthesized second generation polymer PHACOS. One of the peculiarities of this naturally produced bacterial polyester is the presence of thioester groups in the side chain of the polymer. We have shown that thioester groups play a crucial role in polymer activity against *S. aureus*. Related to this, we demonstrate the unique property of this *Pseudomonas putida* biopolyester to be active against other bacterial species. Nevertheless, further modification of PHACOS for fine tuning of its activity and specific applications could be easily achieved using its functionalized side chains to incorporate different active molecules. In addition, we observed a clear inhibition of *S. aureus* biofilm development on PHACOS.

It has been estimated that biofilms are associated with 65% of nosocomial infections [31]. Biofilm formation on biomaterials can generally be divided into two main stages: bacterial adhesion, which depends on surface properties of both substrate and cells, and increase of biofilm mass, which depends on initial attachment and specific growth rate of attached cells [25]. Mauclaire et al. [25] provided an evaluation for the potential of pathogenic biofilm development on non-functionalized mcl-PHAs showing better attachment of *Escherichia coli* to mcl-PHA coatings than *S. aureus*. Moreover, impurity elimination of the biopolyester coating drastically limits biofilm formation [25]. A significant correlation was observed between bacterial attachment and roughness for *S. aureus*, a bacterium which is known to be sensitive to surface irregularities [32]. Although PHACOS shows higher roughness than PHO (data not shown) no increase in attachment of *S. aureus* cells to PHACOS was

observed. Moreover, *S. aureus*^{T} biofilm formation was decreased on PHACOS when compared to PHO.

Novel approaches for the development of antimicrobial polymers are an important area of research and many reports have been published referring to the synthesis of macromolecules that are inherently antimicrobial (biocidal polymers). These are usually positively charged macromolecules that interact with microbial cells that generally carry a negative net charge at the surface due to their membrane proteins, teichoic acids of Gram-positive bacteria, and negatively charged phospholipids at the outer membrane of Gram-negative bacteria. Cationic polymers, biocide-releasing polymers and antimicrobial peptides have been the main focus (for reviews, see Refs. [7,30,33,34]). These subjects have attracted much attention and significant improvements in understanding of their essential physiochemical properties and mode of action have been made. To date neither the antibacterial activity of PHAs nor their anti-adherent properties on bacteria were reported. However, a low, but definite, antibacterial activity of monomers derived from PHAs (*R*-3-hydroxycarboxylic acids) has been demonstrated [35,36].

This work suggests that PHACOS acts as contact active surface and therefore could be considered as biocidal polymer. However, taking into account the notable antibacterial activity of 6-acetylthiohexanoic acid, we cannot discard the possibility that its hydroxyl-derivates (monomers) may be the real polymeric biocide, as the polymerization of active monomeric units leads to an antimicrobial polymer, although we have not observed any *in vitro* degradation of the polymer, at least during one month (data not shown). In this respect, a homopolymer of thioester monomers would be preferable to reach the maximum antimicrobial activity of PHACOS material. The composition of the biopolymer in terms of incorporation of functionalized or non-functionalized monomers can be fully controlled by the bacterium culture conditions and by engineering the metabolic and regulatory networks of *P. putida.* Presently, some gene transcription regulatory restrictions cannot be avoided and non-substituted fatty acids must be added to the culture medium for PHACOS accumulation [13]. It is expected that the more antimicrobial thioester ligands linked to the polyester back bone, the more effective biocide activity of PHACOS. However, the percentage of thioester monomers in the polymer used in this study is already 77% and no activity was observed against other bacteria than *S. aureus.*

Several antibacterial polymers are known to be selective against *S. aureus* over other species. Cationic polymers including poly-norbornenes [37], oligolysins [38], and chitosan [39] all showed selective activity against *S. aureus* over *E. coli*. Although the chemical structures of these polymers are quite different from each other, the cationic functionality appears to be in common, which may be the key determinant in the activity against *S. aureus*. Recently, Gibney et al. demonstrated that commercially available unmodified polyethyleneimines (PEIs) with branched structures (M_r = 500–12,000) are antibacterial with superior activity against *S. aureus* than against *E. coli* [40]. The finding that the single strain of *Staphylococcus epidermidis* tested, *i.e.*, the type strain, was not killed by PHACOS may be explained by a strain-specific effect or, most probably, by differences between *S. aureus* and *S. epidermidis*. Notably, *S. epidermidis* (but not *S. aureus*) produces a surface-attached polymer (poly-γ-DL-glutamic acid) that protects the bacterium from antimicrobial peptides and neutrophil phagocytosis [41]. Whether the presence of this polymer may be involved in the PHACOS resistance of coagulase-negative staphylococci (e.g., *S. epidermidis*) warrants further studies. The mode of action of certain polymers has been studied and defined [42–44]. Nevertheless, the precise mechanism(s) by which PHACOS decrease biofilm formation and kills bacteria is still a matter of debate. The recent review of Timofeeva et al. [45] thoroughly discusses the influence of relevant parameters, such as molecular weight, type and degree of alkylation, and distribution of charge on the

bactericidal action of antimicrobial polymers. Therefore, there are many factors that should be investigated to unravel the mode of action of PHACOS.

Apart from the desirable antimicrobial properties, low inflammation is essential for the acceptance of an incorporated object by mammals [46]. Tests have shown that PHAs provoke mild host reactions when implanted, which is not surprising when considering the fact that [*R*]-3-hydroxybutyric acid is a normal constituent of blood at concentrations between 0.3 and 1.3 mM [47] and is also found in the cell envelope of eukaryotes [48]. Many successful studies using various animal models have clearly demonstrated that PHA, represented by poly(3-hydroxybutyrate), copolymer of 3-hydroxybutyrate and 3-hydroxyvalerate, poly(4-hydroxybutyrate), poly[*R*]-3-hydroxyoctanoate (PHO) and copolymers of 3-hydroxybutyrate and 3-hydroxyhexanoate, possesses the biodegradability, thermoprocessibility and induce low inflammation and therefore are suitable for implant applications [9]. However, very few of naturally functionalized bacterial polyesters have been tested as biomaterials [49]. The biomedical applications of PHO and other mcl-PHAs have been recently reviewed [12]. Here we present results from an *in vivo* study on PHACOS antimicrobial activity and good host acceptance in terms of inflammatory response.

5. Conclusions

We describe a new and unexpected property of PHACOS, a second generation biopolymer, showing antibacterial activity specifically against *S. aureus* isolates including MRSA and decreasing *S. aureus*^{T} biofilm formation. This ability has been ascribed to the functionalized side chains containing thioester groups. Furthermore, we show the possibility of PHACOS for biomedical applications as an implant material demonstrating its antimicrobial properties and minimal inflammation *in vivo*.

Supplementary Material

Refer to Web version on PubMed Central for supplementary material.

Acknowledgments

N.D. is a fellow of JAE Pre-doc Program of CSIC. M.F.-G. and F.P-R thank the program JAE DOC of the CSIC for financial support. The technical works of A. Valencia and F. de la Peña are greatly appreciated. We are indebted to Biópolis S.L. for the supplied polymers. This work was supported by the Ministerio of Economía y Competitividad (BIO2010-21049), the U.S.A. National Institutes of Health grant R21 AI094624 (A.J.G.), the Georgia Tech/Emory Center for the Engineering of Living Tissues, the Atlanta Clinical and Translational Science Institute under PHS Grant UL RR025008 from the Clinical and Translational Science Award Program. Financial support from the CIBER-BBN is acknowledged. CIBER de Enfermedades Respiratorias (CIBERES) is an initiative of Instituto de Salud Carlos III (ISCIII).

References

1. Kiedrowski MR, Horswill AR. New approaches for treating staphylococcal biofilm infections. Ann N Y Acad Sci. 2011; 1241:104–21. [PubMed: 22191529]
2. DeLeo FR, Chambers HF. Reemergence of antibiotic-resistant *Staphylococcus aureus* in the genomics era. J Clin Invest. 2009; 119:2464–74. [PubMed: 19729844]
3. Darouiche RO. Treatment of infections associated with surgical implants. N Engl J Med. 2004; 350:1422–9. [PubMed: 15070792]
4. Grundmann H, Aires-de-Sousa M, Boyce J, Tiemersma E. Emergence and resurgence of meticillin-resistant *Staphylococcus aureus* as a public-health threat. Lancet. 2006; 368:874–85. [PubMed: 16950365]

5. Klein E, Smith DL, Laxminarayan R. Community-associated methicillin-resistant *Staphylococcus aureus* in outpatients, United States, 1999–2006. Emerg Infect Dis. 2009; 15:1925–30. [PubMed: 19961671]
6. Cornell RJ, Donaruma LG. 2-Methacryloxytropones. Intermediates for the synthesis of biologically active polymers. J Med Chem. 1965; 8:388–90. [PubMed: 14323155]
7. Siedenbiedel F, Tiller JC. Antimicrobial polymers in solution and on surfaces: overview and functional principles. Polymers. 2012; 4:46–71.
8. Gomes ME, Reis RL. Biodegradable polymers and composites in biomedical applications: from catgut to tissue engineering. Part 1. Available systems and their properties. Int Mater Rev. 2004; 49:261–73.
9. Chen G-Q, Wu Q. The application of polyhydroxyalkanoates as tissue engineering materials. Biomaterials. 2005; 26:6565–78. [PubMed: 15946738]
10. Chen GQ. A microbial polyhydroxyalkanoates (PHA) based bio- and materials industry. Chem Soc Rev. 2009; 38:2434–46. [PubMed: 19623359]
11. Steinbüchel A, Valentin HE. Diversity of bacterial polyhydroxyalkanoic acids. FEMS Microbiol Lett. 1995; 128:219–28.
12. Hazer DB, Kılıçay E, Hazer B. Poly(3-hydroxyalkanoate)s: diversification and biomedical applications. A state of the art review. Mater Sci Eng C. 2012; 32:637–47.
13. Escapa IF, Morales V, Martino VP, Pollet E, Avérous L, García JL, et al. Disruption of β-oxidation pathway in *Pseudomonas putida* KT2442 to produce new functionalized PHAs with thioester groups. Appl Microbiol Biotechnol. 2011; 89:1583–98. [PubMed: 21267558]
14. Furrer P, Panke S, Zinn M. Efficient recovery of low endotoxin medium-chain-length poly([*R*]-3-hydroxyalkanoate) from bacterial biomass. J Microbiol Methods. 2007; 69:206–13. [PubMed: 17316850]
15. FDA. U.S. Department of Health and Human Services FaDA. Guideline on validation of the Limulus amebocyte lysate test as an end-product endotoxin test for human an animal parenteral drugs, biological products, and medical devices. Rockville, MD: 1987. http://www.gmpua.com/Validation/Method/LAL/FDAGuidelineForTheValidationA.pdf
16. Moscoso M, García E, López R. Biofilm formation by *Streptococcus pneumoniae*: role of choline, extracellular DNA, and capsular polysaccharide in microbial accretion. J Bacteriol. 2006; 188:7785–95. [PubMed: 16936041]
17. Sambrook, J.; Russell, DW. A laboratory manual. Cold Spring Harbor, New York: Cold Spring Harbor Laboratory Press; 2001. Molecular cloning.
18. CLSI. Methods for dilution antimicrobial susceptibility tests for bacteria that grow aerobically, document M07-A8. Wayne, PA: Clinical and Laboratory Standards Institute; 2008.
19. Mosmann T. Rapid colorimetric assay for cellular growth and survival: application to proliferation and cytotoxicity assays. J Immunol Methods. 1983; 65:55–63. [PubMed: 6606682]
20. Wang S-Y, Lan X-Y, Xiao J-H, Yang J-C, Kao Y-T, Chang S-T. Antiinflammatory activity of *Lindera erythrocarpa* fruits. Phytother Res. 2008; 22:213–6. [PubMed: 17726736]
21. Schmidt, HHW.; Kelm, M. Determination of nitrite and nitrate by the Griess reaction. In: Feelisch, M.; Stamler, JS., editors. Methods in nitric oxide research. Chichester, UK: Wiley; 1996. p. 491-7.
22. Kundu K, Knight SF, Willett N, Lee S, Taylor WR, Murthy N. Hydrocyanines: a class of fluorescent sensors that can image reactive oxygen species in cell culture, tissue, and in vivo. Angew Chem Int Ed Engl. 2009; 48:299–303. [PubMed: 19065548]
23. National Research Council. United States Department of Health and Human Services PHS, National Institutes of Health. Committee on care and use of laboratory animals of the Institute of Laboratory Animal Resources, Commission on life sciences. Bethesda, MD: National Research Council; 1985. Guide for the care and use of laboratory animals. NIH Publication No. 85–23
24. Selvam S, Kundu K, Templeman KL, Murthy N, García AJ. Minimally invasive, longitudinal monitoring of biomaterial-associated inflammation by fluorescence imaging. Biomaterials. 2011; 32:7785–92. [PubMed: 21813173]
25. Mauclaire L, Brombacher E, Bünger JD, Zinn M. Factors controlling bacterial attachment and biofilm formation on medium-chain-length polyhydroxyalkanoates (mcl-PHAs). Colloids Surf B Biointerfaces. 2010; 76:104–11. [PubMed: 19914047]

26. Kojima M, Morisaki T, Izuhara K, Uchiyama A, Matsunari Y, Katano M, et al. Lipopolysaccharide increases cyclo-oxygenase-2 expression in a colon carcinoma cell line through nuclear factor-κB activation. Oncogene. 2000; 19:1225–31. [PubMed: 10713711]
27. Lin PW, Myers LES, Ray L, Song S-C, Nasr TR, Berardinelli AJ, et al. *Lactobacillus rhamnosus* blocks inflammatory signaling in vivo via reactive oxygen species generation. Free Radic Biol Med. 2009; 47:1205–11. [PubMed: 19660542]
28. Zimmerli W, Trampuz A, Ochsner PE. Prosthetic-joint infections. N Engl J Med. 2004; 351:1645–54. [PubMed: 15483283]
29. Butler MS, Cooper MA. Antibiotics in the clinical pipeline in 2011. J Antibiot. 2011; 64:413–25. [PubMed: 21587262]
30. Kuroda K, Caputo GA. Antimicrobial polymers as synthetic mimics of host-defense peptides. Wiley Interdiscip Rev Nanomed Nanobiotechnol. 2013; 5:49–66. [PubMed: 23076870]
31. Mah T-FC, O'Toole GA. Mechanisms of biofilm resistance to antimicrobial agents. Trends Microbiol. 2001; 9:34–9. [PubMed: 11166241]
32. Harris LG, Richards RG. Staphylococci and implant surfaces: a review. Injury. 2006; 37:S3–14. [PubMed: 16651069]
33. Lejars M, Margaillan A, Bressy C. Fouling release coatings: a nontoxic alternative to biocidal antifouling coatings. Chem Rev. 2012; 112:4347–90. [PubMed: 22578131]
34. Wang, Y.; Schanze, KS.; Chi, EY.; Whitten, DG. When worlds collide: interactions at the interface between biological systems and synthetic cationic conjugated polyelectrolytes and oligomers. Langmuir. 2013. http://dx.doi.org/10.1021/la4012263
35. Sandoval Á, Arias-Barrau E, Bermejo F, Cañedo L, Naharro G, Olivera ER, et al. Production of 3-hydroxy-*n*-phenylalkanoic acids by a genetically engineered strain of *Pseudomonas putida*. Appl Microbiol Biotechnol. 2005; 67:97–105. [PubMed: 15800732]
36. Ruth K, Grubelnik A, Hartmann R, Egli T, Zinn M, Ren Q. Efficient production of (*R*)-3-hydroxycarboxylic acids by biotechnological conversion of polyhydroxyalkanoates and their purification. Biomacromolecules. 2006; 8:279–86. [PubMed: 17206818]
37. Lienkamp K, Madkour AE, Musante A, Nelson CF, Nüsslein K, Tew GN. Antimicrobial polymers prepared by ROMP with unprecedented selectivity: a molecular construction kit approach. J Am Chem Soc. 2008; 130:9836–43. [PubMed: 18593128]
38. Epand RF, Sarig H, Mor A, Epand RM. Cell-wall interactions and the selective bacteriostatic activity of a miniature oligo-acyl-lysyl. Biophys J. 2009; 97:2250–7. [PubMed: 19843457]
39. Raafat D, von Bargen K, Haas A, Sahl HG. Insights into the mode of action of chitosan as an antibacterial compound. Appl Environ Microbiol. 2008; 74:3764–73. [PubMed: 18456858]
40. Gibney KA, Sovadinova I, Lopez AI, Urban M, Ridgway Z, Caputo GA, et al. Poly(ethylene imine)s as antimicrobial agents with selective activity. Macromol Biosci. 2012; 12:1279–89. [PubMed: 22865776]
41. Otto M. Molecular basis of *Staphylococcus epidermidis* infections. Semin Immunopathol. 2012; 34:201–14. [PubMed: 22095240]
42. Olofsson A-C, Hermansson M, Elwing H. *N*Acetyl-L-cysteine affects growth, extracellular polysaccharide production, and bacterial biofilm formation on solid surfaces. Appl Environ Microbiol. 2003; 69:4814–22. [PubMed: 12902275]
43. Pérez-Giraldo C, Rodríguez-Benito A, Morán FJ, Hurtado C, Blanco MT, Gómez-García AC. Influence of *N*-acetylcysteine on the formation of biofilm by *Staphylococcus epidermidis*. J Antimicrob Chemother. 1997; 39:643–6. [PubMed: 9184365]
44. Hernandez MD, Mansouri MD, Aslam S, Zeluff B, Darouiche RO. Efficacy of combination of *N*-acetylcysteine, gentamicin, and amphotericin B for prevention of microbial colonization of ventricular assist devices. Infect Control Hosp Epidemiol. 2009; 30:190–2. [PubMed: 19090771]
45. Timofeeva L, Kleshcheva N. Antimicrobial polymers: mechanism of action, factors of activity, and applications. Appl Microbiol Biotechnol. 2011; 89:475–92. [PubMed: 20953604]
46. Zinn M, Witholt B, Egli T. Occurrence, synthesis and medical application of bacterial polyhydroxyalkanoate. Adv Drug Deliv Rev. 2001; 53:5–21. [PubMed: 11733115]

47. Wiggam MI, O'Kane MJ, Harper R, Atkinson AB, Hadden DR, Trimble ER, et al. Treatment of diabetic ketocidosis using normalization of blood 3-hydroxybutyrate concentration as the endpoint oemergency management. A randomized controlled study. Diabetes Care. 1997; 20:137–52.

48. Reusch RN. Transmembrane ion transport by polyphosphate/poly-(R)-3-hydroxybutyrate complexes. Biochemistry (Mosc). 2000; 65:280–95. [PubMed: 10739470]

49. Tortajada M, da Silva FL, Prieto MA. Secon-generation functionalized médium-chain-length polyhydroxyalkanoates: th gateway to high-value bioplastic applications. Int Microbiol. 2013; 16:1–15. [PubMed: 24151777]

Appendix A. Supplementary data

Supplementary data related to this article can be found at http://dx.doi.org/10.1016/j.biomaterials.2013.09.059.

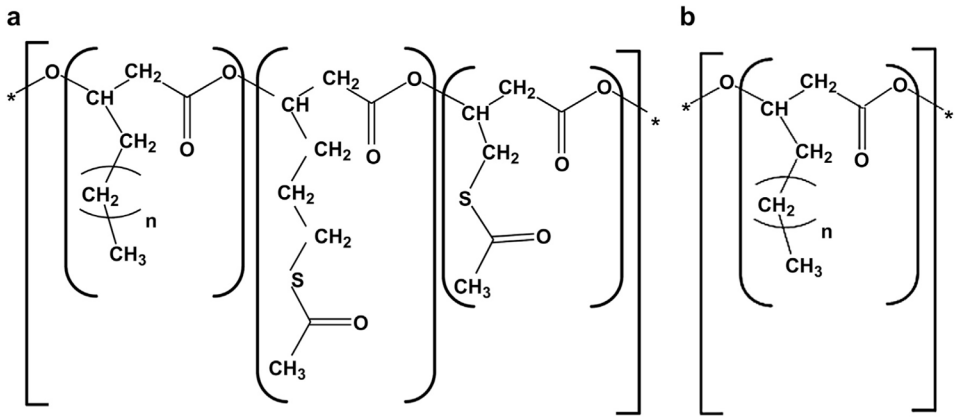

Fig. 1.

Schematic representation of medium chain length PHAs chemical structure. (a) poly(3-hydroxy-6-acetylthiohexanoateco-4-acetylthiobutanoate) PHACOS composed of functionalized (3-hydroxy-6-acetylthiohexanoate and 3-hydroxy-4-acetylthiobutanoate monomers) and of non-functionalized monomers (3-hydroxyoctanoate, 3-hydroxydecanoate, and traces of 3-hydroxyhexanoate monomers). (b) poly(3-hydroxyoctanoate-*co*-hydroxyhexanoate) PHO composed of non-functionalized monomers (3-hydroxyoctanoate and 3-hydroxyhexanoate monomers).

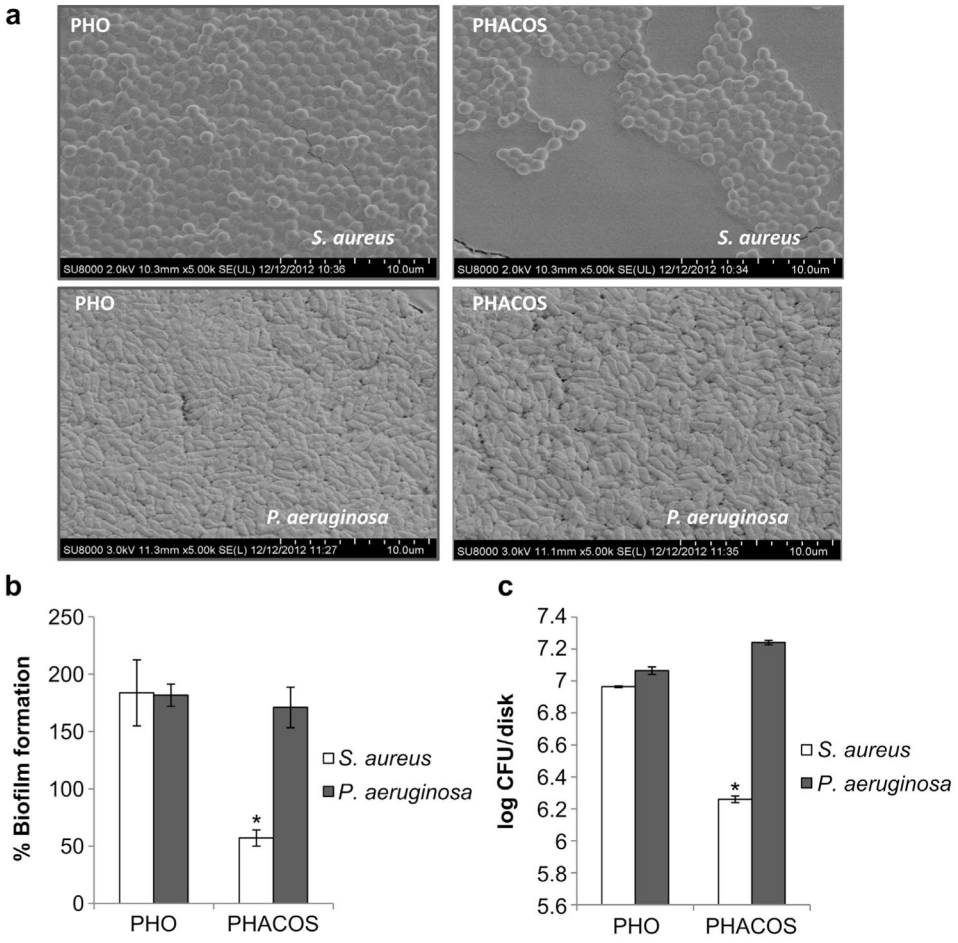

Fig. 2.

PHACOS and PHO disks and biofilm formation. (a) ESEM of *S. aureus*^{T} and *P. aeruginosa* biofilms. (b) Crystal violet staining assay for biofilm quantification. The capacity of biofilm formation on control PET disks is considered 100%. (c) Bacterial viability, CFU counts.

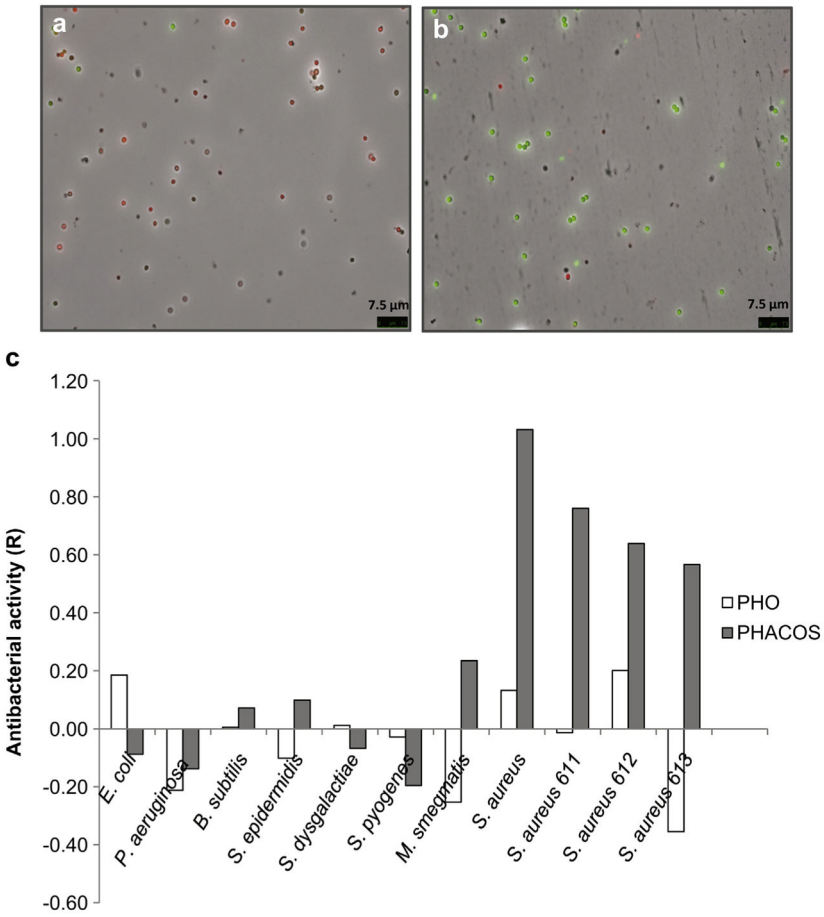

Fig. 3.

Comparison of antiadherent and antibacterial activities of PHACOS and PHO surfaces on *S. aureus*^{T}. Fluorescence microscopy using Bacterial Viability test on PHACOS (a) and PHO (b). (c) Measurement of antibacterial activity of polymer (PHACOS and PHO) surfaces. *R* = 1 means 10-fold less viable cells recovered from sample disk after 24 h when compared to the control disk. The ISO 22196:2011 stated conditions were fully satisfied in term of statistics.

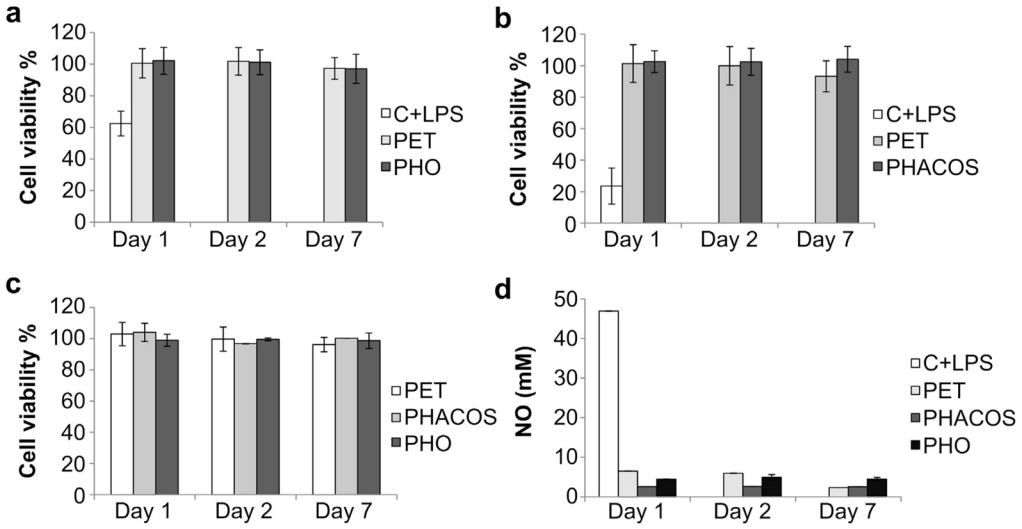

Fig. 4.

In vitro determination of PHACOS and PHO cytotoxicity and immunocompatibility. (a) Determination of PHO cytotoxic effect on mouse RAW 264.7 macrophages by MTT assay. Negative control extracts were incubated with PET disks. Positive control cells were treated with LPS to monitor the decrease in cell viability. (b) Determination of PHACOS cytotoxic effect on RAW 264.7 macrophages. (c) Determination of PHO and PHACOS cytotoxic effect on mouse fibroblasts (BALB 3T3). Control extracts were incubated with PET disks. (d) Griess test. Inflammatory activity of PHACOS and PHO on RAW 264.7 macrophages measured as increase of NO production, Open, light gray, dark gray, and black bars represent, respectively, positive control (cells treated with LPS), negative control (extracts incubated with PET), incubated with PHACOS, incubated with PHO.

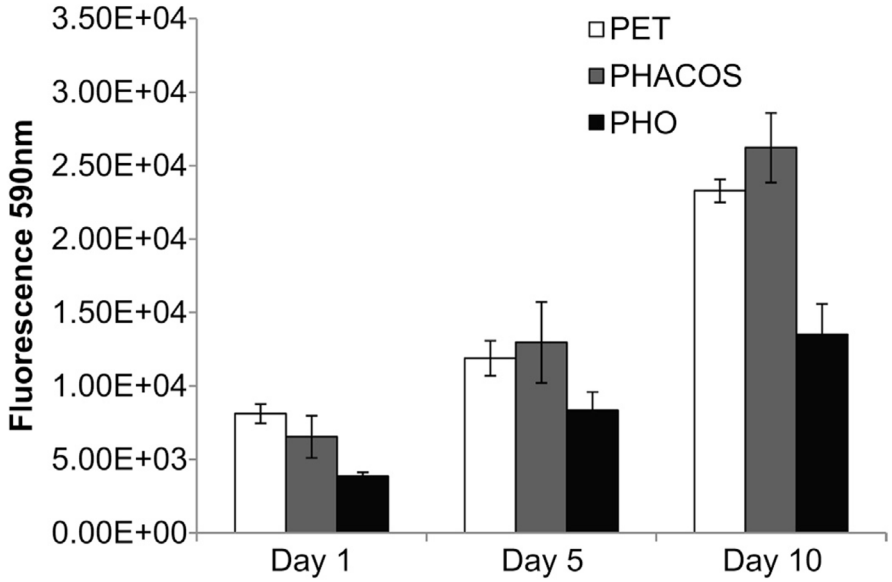

Fig. 5.
AB assay for determination of BALB 3T3 fibroblasts *in vitro* proliferation on PHACOS (gray bars) and PHO surfaces (black bars). White bars represent PET control.

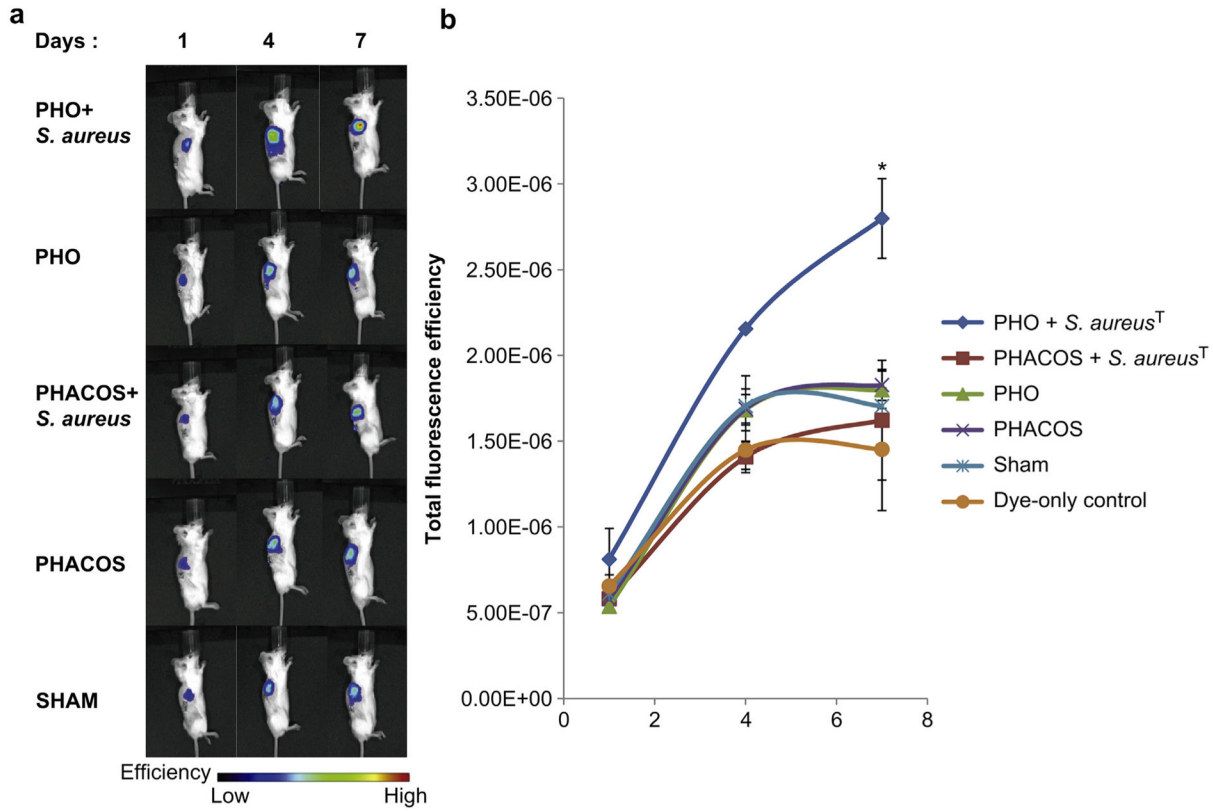

Fig. 6.

In vivo ROS imaging of PHACOS and PHO implant-associated inflammation after subcutaneous administration of H-ICG. (a) Bioimaging data of animals. (b) Quantification of bioimaging ROS fluorescence data of mice with PHACOS and PHO implants incubated with *S. aureus*^{T} and sterile PHACOS and PHO implants (*$P < 0.05$ between sham and implant, $n > 3$ mice/time point for sham and implant groups).

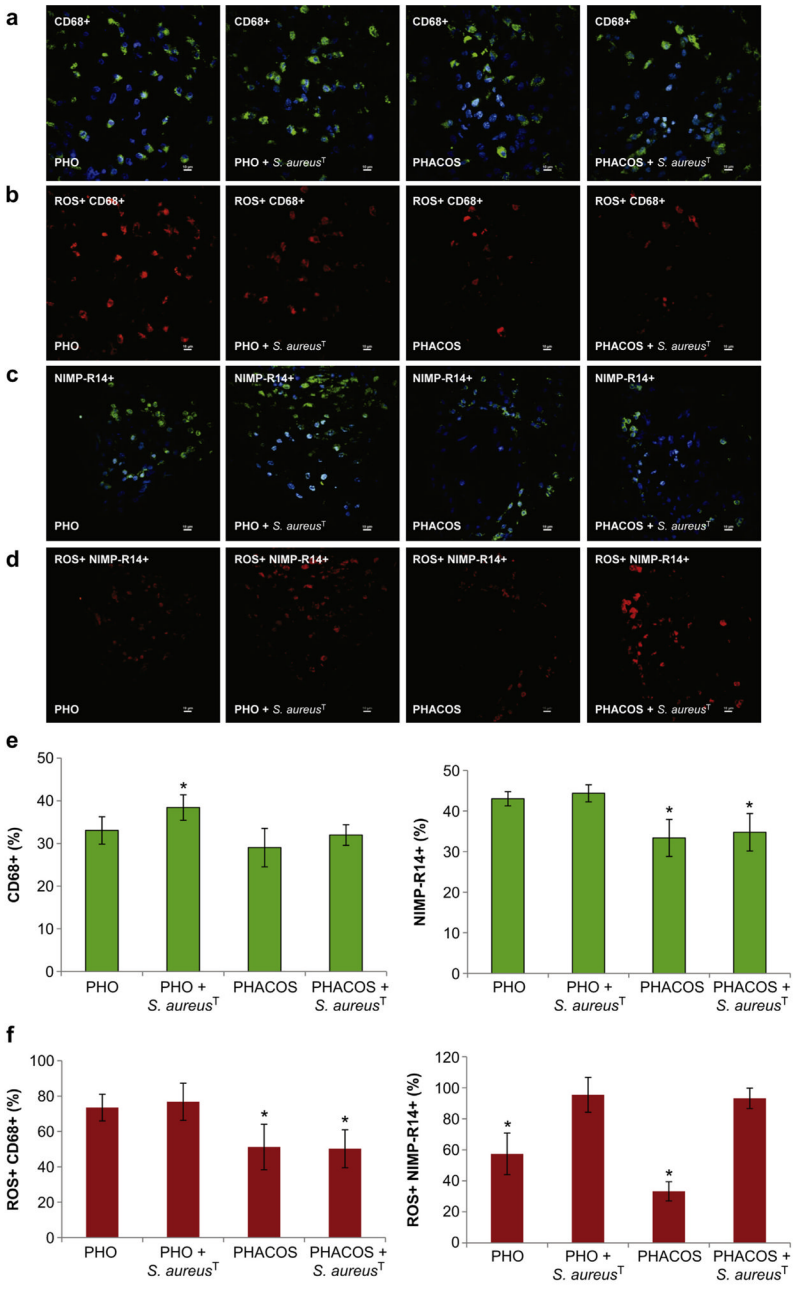

Fig. 7.

Immunohistochemical staining for macrophages and neutrophils in implant-associated inflammation. (a) Representative co-localization images of macrophages (CD68$^+$; green) and nuclei (DAPI; blue) in 14-d: sterile PHO; *S. aureus*^{T} precolonized PHO; sterile PHACOS; *S. aureus* precolonized PHACOS implants (from left to right). (b) Intracellular ROS (H-Cy5+, red) co-localizing with macrophages in: sterile PHO; *S. aureus*^{T} pre-colonized PHO; sterile PHACOS; *S. aureus*^{T} pre-colonized PHACOS implants (from left to right). (c) Neutrophils (NIMP-R14$^+$; green) with DAPI in 14-d: sterile PHO; *S. aureus* precolonized PHO; sterile PHACOS; *S. aureus*^{T} precolonized PHACOS implants. (d) Intracellular ROS (H-Cy5+, red) co-localizing with neutrophils in: sterile PHO; *S. aureus*^{T} pre-colonized PHO; sterile PHACOS; *S. aureus*^{T} pre-colonized PHACOS implants (from

left to right). (e) Quantification of $CD68^+$ (left) and NIMP-R14 cells (right) stained positive for $CD68^+$ (macrophages) and for NIMP-$R14^+$ cells (neutrophiles) ($n = 3$ mice/time point; $*P < 0.05$ between macrophage recruitment to *S. aureus*^{T} pre-colonized PHO and *S. aureus*^{T} pre-colonized PHACOS implant; neutrophil recruitment to sterile PHO and sterile PHACOS implants; neutrophil recruitment to *S. aureus*^{T} pre-colonized PHO and *S. aureus*^{T} pre-colonized PHACOS). (f) Quantification of $CD68^+$ and ROS^+ (left) and NIMP-R14 and ROS^+ (right) cells co-localization ($n = 3$ mice/time point; $*P < 0.05$ between ROS active macrophage on sterile PHO and sterile PHACOS implant; ROS active macrophage on *S. aureus*^{T} pre-colonized PHO and *S. aureus*^{T} pre-colonized PHACOS implant; ROS active neutrophil on sterile PHO and *S. aureus*^{T} pre-colonized PHO; ROS active neutrophil on sterile PHACOS and *S. aureus*^{T} pre-colonized PHACOS implant).

Table 1

Bacterial strains used in this study.

Bacteria[a]	Origin/characteristics[b]
Staphylococcus aureus subsp. *aureus*^{T}	CECT 86
Mycobacterium smegmatis^T	CECT 3020
Escherichia coli	CECT 516
Pseudomonas aeruginosa PAO1	CECT 4122
Staphylococcus epidermidis^T	CECT 232
Bacillus subtilis subsp. *subtilis*	CECT 39
Streptococcus dysgalactiae subsp. *equisimilis*	CECT 926
Streptococcus pyogenes	CECT 985
Staphylococcus aureus 61115	A. Vindel, ISCIII/MRSA
Staphylococcus aureus 61286	A. Vindel, ISCIII/MRSA
Staphylococcus aureus 61314	A. Vindel, ISCIII/MRSA

[a] ^{T}, type strain.

[b] CECT, Colección Española de Cultivos Tipo; ISCIII, Instituto de Salud Carlos III; MRSA, methicillin-resistant *Staphylococcus aureus* (clinical isolate).